

Atomic Talbot interferometry as a sensitive tool for cavity quantum electrodynamics

B. Rohwedder* and M. França Santos

Instituto de Física, Universidade Federal do Rio de Janeiro, Caixa Postal 68.528, 21945-970 Rio de Janeiro, RJ, Brazil

(Received 6 July 1999; published 6 January 2000)

Atomic Talbot interferometry is shown to be potentially useful both for the experimental determination of arbitrary electromagnetic cavity photon number distributions and for the demonstration of the quantum nature of nearly classical light fields.

PACS number(s): 03.75.Be, 39.20.+q, 42.50.Vk, 03.65.Bz

I. INTRODUCTION

Technical advances in the field of cavity quantum electrodynamics have led to the possibility of demonstrating some of the most fundamental predictions of quantum theory in systems so simple that experiments formerly considered to be merely of the “gedanken” type have now become actually feasible. In addition to providing textbook examples of some basic quantum-mechanical issues, the novel experimental methods have triggered a renewed interest in the conceptual fundamentals of our quantum description of nature. New questions related to quantum measurement theory and the borderline between the classical and the quantum world have been raised. In this paper we address both these questions in terms of two different experimental propositions for the study of the quantum properties of the electromagnetic field inside an optical cavity.

Several authors have shown how atoms crossing the cavity under inspection may be used as efficient probes of the photon distribution inside it [1–9]. Some of the proposed schemes make use of the fact that in the optical regime, the (statistics-dependent) diffraction of atoms off a nearly resonant light field is easily observable, contrary to the microwave regime, where such mechanical effects would be much too small to be detectable. Still, the fact that the measured diffraction pattern depends on the quantum properties of the scattering field does not imply that its statistics can be read off simply and unambiguously. In Ref. [9], for instance, it is shown that the atomic near-field diffraction patterns produced behind a far-off detuned (quantized) standing light wave may contain all, or absolutely no, information about the governing photon statistics, depending on the distance at which they are observed. Although it is, in principle, simple and straightforward to extract from the detected atomic spatial distribution (measured at some proper distance behind the light field) all information needed for the determination of the photon statistics, the practical implementation of such a scheme is technically difficult due to the required high spatial detector resolution. If, on the contrary, the atoms are observed in the far field, resolution requirements become less severe, but the need to detect all diffraction orders in order to reconstruct the light field statistics again makes such a scheme impractical. In addition, far-field approaches do not generally allow a simple deconvolution of the information

stored in the arising diffraction pattern.

A viable compromise may be achieved using the Talbot interferometrical setup, which is the subject of the present paper. In this scheme a second, but classical (laser), standing light wave is introduced as shown in Fig. 1. If the atomic flux diffracted into the zeroth (far-field diffraction) order is measured while the intensity of the laser is varied, information on the quantum field is gained. Although the way this information must be retrieved from the data is, from a theoretical point of view, less satisfactory than in a near-field approach, the relative simplicity of the method, from an experimental point of view, makes it a better candidate for an actual realization.

A particularly interesting aspect of our scheme is that it can also be used to null-test the quantization of electromagnetic fields, even if substantially more than just a few photons are involved. While unambiguous experimental demonstrations of light quantization exist in some few-photon systems [10], the quantum nature of a macroscopic field is difficult to prove due to the correspondence principle. A “quantum lens” originally proposed to demonstrate photon discreteness even in the classical limit [11] turned out not to serve this purpose [12] because of a general tendency, in this limit, of quantum features to get washed out. Our way around this problem consists of considering a situation in which the correspondence principle predicts a vanishing measuring result. If an experiment reports a *nonzero* result, this would indicate that quantum mechanics is at play. In any realistic experiment, however, different sources of aberration

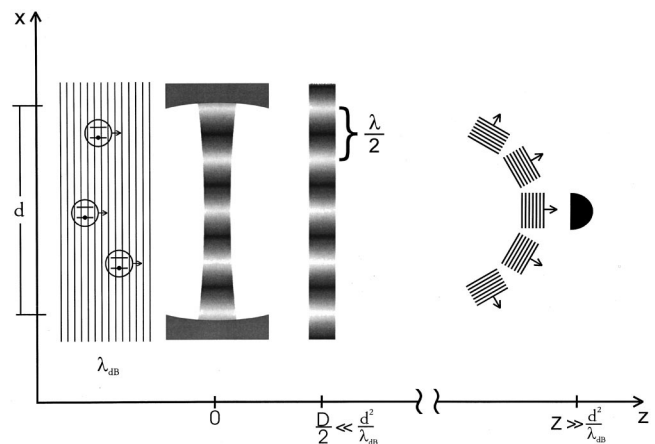


FIG. 1. Basic scheme of the proposed atomic Talbot interferometer. The atoms are detected in the diffraction far-field.

*Electronic address: bernd@if.ufrj.br

can mimic a quantum signature of the analyzed light field. It is thus necessary to identify these sources in order to estimate their influence and to visualize ways to get them under control.

The paper is organized as follows. First, in Sec. II, the concept of Talbot interferometry will be introduced, with special emphasis on its atom-optical realization. In Sec. III, far-field diffraction off a quantized light grating will be studied with and without a second, classical light field in place. Section IV discusses how a quantum nondemolition (QND) measurement could be performed with the described apparatus. Section V is devoted to the detection of a quantum signature (without an actual measurement of the photon statistics) when a ‘‘macroscopic’’ field is being analyzed. Finally, in Sec. VI, we try to identify the most important sources of aberrations, estimate their importance, and propose ways to eventually circumvent them.

II. TALBOT INTERFEROMETRY

Moiré fringes are an optical phenomenon that arises when the shadows of two or more consecutive gratings superpose. Quite generally, geometrical shadows are expected when the light wavelength is substantially smaller than the involved grating constants. As these are reduced, diffraction effects start to become increasingly apparent, and simple shadows will only be expected in the proximities immediately behind a grating. However, in a first-order approximation beyond geometrical optics, a notable exception shows up. In addition to the expected proper shadows at short distances $z \ll D$ behind the grating, where D is the fundamental *Talbot length*

$$D = \frac{2\lambda_x^2}{\lambda_z} \quad (1)$$

and λ_x and λ_z denote the grating constant and the wavelength, respectively, additional ‘‘shadows’’ (self-images) of the grating emerge at integral and half-integral [13] multiples of D . Since it was discovered in 1836 [14], this *Talbot effect* has been extensively studied and applied. A concise introduction and overview can be found in Refs. [15,16]. For our present purposes it is enough to know that a pair of identical gratings separated from each other by a distance D (or $D/2$) can produce Moiré-like fringes even in a domain where diffraction dominates. We note that at other intermediate distances the diffraction patterns can become arbitrarily complex, and do not lend themselves to such a simple picture. It must also be emphasized that, since D depends on the wavelength, in order to observe Moiré fringes in a diffraction-dominated regime a well-monochromatized source is mandatory. For an isotopically pure atomic beam, this implies that from now on we will assume that its velocity distribution has been sufficiently compressed around some average value v_z .

That a pair of gratings separated by D (or $D/2$) can be used for interferometrical purposes was first pointed out and demonstrated by Lohmann and Silva [17]. A series of applications of these optical *Talbot interferometers* (TIs) are discussed in [15]. If light waves are replaced by atomic de Broglie waves and the grating period is correspondingly

scaled down, one obtains the *atomic* TI introduced in [18,19] and thoroughly analyzed in Ref. [20]. We will skip a further discussion of this kind of TI because they all use *amplitude* gratings, which will not be the subject of the present paper. On the contrary, and as we will briefly derive in the next section, a standing light wave which is strongly detuned from a given atomic transition acts as a pure phase grating for atoms. Far-field diffraction from such a grating made of light was demonstrated in Refs. [21,22]. To date, and to our knowledge, a corresponding study of the near field and its self-imaging phenomena has not been reported.

The Moiré and Talbot effects do not depend on the specific nature of the gratings producing them. In order to visualize this, let us consider the two above-mentioned most common gratings in current atom optics. The transmission function of a microfabricated grating with open fraction 1/2, for instance, is the periodic repetition, $T(x) = T(x + \lambda_x)$, of the unit cell

$$T(x) = \begin{cases} 0 & \text{for } -\lambda_x/2 \leq x < 0 \\ 1 & \text{for } 0 \leq x < \lambda_x/2. \end{cases} \quad (2)$$

An identical second grating placed at $z = D/2$ will produce Moiré fringes which depend on the relative displacement of the two diffraction structures. Since the Talbot shadow of the first grating is displaced by half a grating period at this distance, a second grating at this position will absorb all atoms, if unshifted with respect to the entrance grating.

A phase grating, on the contrary, is inherently transparent. Under the circumstances specified in the next section, a standing light wave (wavelength λ) in atom optics is described by a transmission function of the form

$$T(x) = e^{iA \sin^2(2\pi x/\lambda)}, \quad (3)$$

where the numerical constant A depends on the physical parameters of the interaction. Using a terminology reminiscent of ultrasonically produced gratings, we call A the Raman-Nath parameter [15]. Note that the grating period $\lambda_x = \lambda/2$. Such a grating corrugates the incident plane wave by superimposing to it a position-dependent phase. The process can be reversed by placing a second, identical grating at half the Talbot distance behind the first one, as schematized in Fig. 1. Ideally, the decorrugation is perfect and a new plane wave exits the two-grating configuration. If this TI is hidden in a black box, it looks like nothing ever happened to the atomic beam.

In the far field, a single grating may be looked at as a multiple beam splitter. From such a point of view, a phase-grating TI may be seen as a multiple beam interferometer, in which the first grating acts as the splitter and the second one as the beam merger. No mirrors are necessary, since the various diffraction orders are not physically separated at the near-field position of the recombining grating, making this entire picture somewhat artificial. A true multiple beam atom interferometer based on light gratings will be presented elsewhere [23].

III. ATOMIC DIFFRACTION FROM STANDING LIGHT FIELDS

The diffraction of atoms by quantized and classical light fields has been thoroughly studied in previous papers [24]. Our brief introductory presentation here is mainly intended to define the physical situation and our particular notation. In order to reduce the problem to a one-dimensional conservative one, a series of assumptions have to be made. First, the intrinsically three-dimensional spontaneous-emission processes must be eliminated. This can be achieved by detuning the cavity far enough from the atomic resonance frequency and by preparing the atoms in their ground state, in which they will then remain all the time. Second, the atomic velocity v_z along the beam's propagation axis z should be so large that a classical treatment of this motional degree of freedom becomes possible. In essence, this amounts to a parametrization of the coordinate z through the time variable t . If L denotes the interaction length of the cavity [25], this defines an interaction time $t_{\text{int}} \equiv L/v_z$. The only nontrivial dynamics then takes place in the orthogonal x - y plane. If we additionally assume that the system is uniform along y , the "effective" one-dimensional Hamiltonian

$$H_{\text{eff}} \approx \frac{p_x^2}{2M} + \frac{\hbar |g(x)|^2}{\Delta} a^\dagger a \quad (4)$$

provides a good description of the atom-light interaction. Here M is the atomic mass, Δ the detuning, and $g(x)$ the position-dependent coupling with *one* eigenmode of the cavity. Its quantum nature is described by the pair of ladder operators a and a^\dagger , $[a, a^\dagger] = 1$. The precise field geometry inside an optical cavity consisting of a pair of spherical mirrors can be rather complex [26], but under suitable conditions we can approximate the field close to its center by

$$g(x) = g \sin\left(2\pi \frac{x}{\lambda}\right) \quad (5)$$

times a Gaussian-shaped turn on/off in the z direction [25].

We will expand states in terms of the product basis,

$$\sum_{\nu=0}^{\infty} \int_{-\infty}^{\infty} dx' |\nu, x', t\rangle \langle \nu, x', t| = 1, \quad (6)$$

$$\langle \nu, x', t | \mu, x'', t \rangle = \delta_{\nu\mu} \delta(x' - x''), \quad (7)$$

of eigenstates of $a^\dagger a$ and x . Throughout the paper, greek indices will refer to the photon degree of freedom. If an entrance aperture function $f(x)$ is used to describe the shape of the atomic de Broglie wavefront before entering the cavity, which in that instant is assumed to be in an arbitrary state $\sum w_\nu |\nu\rangle$, the initial wave function will be written

$$\langle \nu, x, t = -t_{\text{int}} | \psi \rangle = w_\nu f(x). \quad (8)$$

We define a grating as an optical element which multiplies an incoming wave with a given periodic function T . Then our situation of interest, where the interaction (4) describes a

phase grating for atoms, corresponds to the regime in which the semiclassical approximation $[x, p_x] \approx 0$ can be applied. One then obtains

$$\langle \nu, x, t = 0 | \psi \rangle = w_\nu e^{i\nu(g^2 t_{\text{int}}/\Delta) \sin^2(2\pi x/\lambda)} e^{i(\hbar t_{\text{int}}/2M)(d^2/dx^2)} f(x) \quad (9)$$

for the wave function at the exit of the quantized interaction zone. If the entrance aperture f is smooth and broad enough, the second exponential, which describes the free evolution of the wave function inside the interaction region, may be neglected. Then

$$\langle \nu, x, t = 0 | \psi \rangle \approx \langle \nu, x, t = -t_{\text{int}} | \psi \rangle e^{i\nu(g^2 t_{\text{int}}/\Delta) \sin^2(2\pi x/\lambda)} \quad (10)$$

satisfies our above definition of a grating and the transmission function is of the form (3), with $A = \nu Q$, where

$$Q \equiv \frac{g^2 t_{\text{int}}}{\Delta} \quad (11)$$

is the maximal phase shift per photon. We assume throughout the paper that the value of Q is known by the experimentalist.

In the near field, a wide aperture is also a necessary requirement for the appearance of Talbot self-images. Ideally, a plane entrance wave normalized to unity ($f=1$) propagates freely, after interacting with the grating, according to

$$\langle \nu, x, t > 0 | \psi \rangle = \sqrt{\frac{M}{i2\pi\hbar t}} \int_{-\infty}^{\infty} dx' e^{i[M(x-x')^2/2\hbar t]} T(x'). \quad (12)$$

It is not difficult to show that, in addition to the obvious λ_x periodicity along the x axis, the wave function is D -periodical along the $z = v_z t$ axis, where D is obtained from Eq. (1) by setting λ_z equal to the de Broglie wavelength h/Mv_z . For typical parameters (thermal atom velocities and light grating constants of several 100 nm), D is of the order 10^{-3} to 10^{-2} m.

It is natural to introduce rationalized coordinates ξ, ζ ,

$$x \equiv \lambda_x \frac{\xi}{2\pi}, \quad (13)$$

$$z = v_z t \equiv D \frac{\zeta}{2\pi}, \quad (14)$$

so that the rationalized wave function

$$\psi_\nu(\xi, \zeta) \equiv \left\langle \nu, \lambda_x \frac{\xi}{2\pi}, \frac{D}{v_z} \frac{\zeta}{2\pi} \middle| \psi \right\rangle \quad (15)$$

becomes doubly 2π -periodic. Since typical interaction lengths L satisfy $L \ll D$, for the sake of notational simplicity we will consider the interaction to happen instantaneously

and introduce the convention that, at the light field positions, $\psi_\nu(\xi, \zeta)$ refers to the moment immediately *after* the interaction.

Using this notation, the identity

$$\psi_\nu(\xi, \pi) = \psi_\nu(\xi + \pi, 0) \quad (16)$$

represents the mathematical expression of our previous comment that a shifted shadow of the grating is produced at half the Talbot distance. Equation (16) is a special case of a formula derived in Ref. [16].

In the far field, a wide entrance aperture guarantees spatially well-separated diffraction maxima. Then the intensity $|\psi_j|^2$ of the j th diffraction order is obtained by evaluating the Fourier decomposition of the transmission function, squaring the modulus of the j th Fourier component, and tracing over the photon degree of freedom, explicitly

$$|\psi_j|^2 = \sum_{\nu=0}^{\infty} |w_\nu|^2 J_j^2\left(\frac{\nu Q}{2}\right), \quad (17)$$

where J_j denotes a Bessel function.

In principle, in order to deduce the photon number distribution in the cavity, it would be necessary to measure the intensities of all atomic diffraction orders. In practice, this would be extremely difficult to do. This need may be overcome by adding a second, classical light field at $\zeta = \pi$, i.e., in a TI configuration with respect to the quantum field. As long as the semiclassical approximation that led from Eq. (9) to Eq. (10) may again be applied, the effective Hamiltonian describing the interaction with the classical field reads

$$H_{\text{eff}} = \frac{\hbar G^2}{\Delta} \sin^2\left(\frac{\xi}{2}\right), \quad (18)$$

where G^2 is proportional to the laser intensity. In analogy to the per-photon phase shift Q produced by the quantized field, it is convenient to define the (maximal) phase shift C produced by the classical field as

$$C \equiv \frac{G^2 t_{\text{int}}}{\Delta}. \quad (19)$$

Using Eqs. (10) and (16), the latter implying the approximation $f \approx 1$ to be applicable, we obtain for the wave function after the second interaction

$$\psi_\nu(\xi, \pi) = w_\nu e^{i\nu Q \sin^2(\xi/2)} e^{iC \cos^2(\xi/2)}. \quad (20)$$

In the particular case when the quantum field is in a Fock state $|N\rangle$, a classical field tuned such that $C = NQ$ produces a new plane wave at the exit of this atomic TI. A less trivial case arises when the quantum field is in a coherent state with an average of $N = \langle a^\dagger a \rangle$ photons. Intuitively, for large N one again expects a plane atomic wave emerging from the TI if the condition $C = NQ$ is matched. This conjecture turns out to be true, as will be explicitly shown in Sec. V. Deviations, which (in the absence of other aberrational effects) would be a signature of the quantum nature of the first light field, are best observed in the far field, where they produce measurable

diffraction maxima away from the zeroth order. The far-field diffraction intensities $|\psi_j|^2$ for this TI are a straightforward generalization of Eq. (17),

$$|\psi_j|^2 = \sum_{\nu=0}^{\infty} |w_\nu|^2 J_j^2\left(\frac{\nu Q - C}{2}\right), \quad (21)$$

and correctly reduce to Eq. (17) as $C \rightarrow 0$. For the measurement of the photon number distribution in an arbitrary quantum light field, the presence of the classical light field does not eliminate the in-principle problem that equations of the form (17) and (21) cannot be analytically inverted so as to express the probabilities $|w_\nu|^2$ in terms of the measured diffraction intensities $|\psi_j|^2$. This seems to be a general drawback of far-field approaches, as opposed to near-field methods [9].

The advantage of introducing a classical ‘‘compensating’’ field relies on the fact that the phase shift C can be easily changed by varying the intensity of the autoreflected laser beam. Instead of determining the complete atomic diffraction pattern, it is then only needed to measure the intensity of the undeflected (zeroth order) component while C is scanned over a reasonable interval. This represents an essential experimental simplification. The remaining theoretical problem, the determination of the photon number statistics from the measured dependency of $|\psi_0|^2$ upon C , will be the subject of the following section.

IV. ATOMIC TI AS A QND MEASUREMENT TOOL

Once the dependency of $|\psi_0|^2$ upon the parameter C has been determined experimentally, Eq. (21) can be used to deduce the photon-number distribution inside the cavity. In principle, this could be done by treating the occupation probabilities $|w_\nu|^2$ as fitting parameters to be chosen in such a way that the right-hand side of Eq. (21) matches the measured intensity curve ($j=0$) as well as possible. Under suitable conditions, however, such a clumsy approach turns out to be unnecessary. In fact, if we knew *a priori* that $w_\nu = 0$ for $\nu > n$, then it would be sufficient to measure $|\psi_0|^2$ for $(n+1)$ different values C_0, \dots, C_n of the parameter C , for the set of linear equations

$$\begin{bmatrix} J_0^2\left(\frac{-C_0}{2}\right) & J_0^2\left(\frac{Q-C_0}{2}\right) & \dots & J_0^2\left(\frac{nQ-C_0}{2}\right) \\ \vdots & \vdots & \ddots & \vdots \\ J_0^2\left(\frac{-C_n}{2}\right) & J_0^2\left(\frac{Q-C_n}{2}\right) & \dots & J_0^2\left(\frac{nQ-C_n}{2}\right) \end{bmatrix} \begin{bmatrix} |w_0|^2 \\ |w_1|^2 \\ \vdots \\ |w_n|^2 \end{bmatrix} = \begin{bmatrix} |\psi_0(C_0)|^2 \\ |\psi_0(C_1)|^2 \\ \vdots \\ |\psi_0(C_n)|^2 \end{bmatrix} \quad (22)$$

can be solved by matrix inversion. For two practical reasons a much larger number of measuring points will have to be determined, though. First, we do in general lack a previous

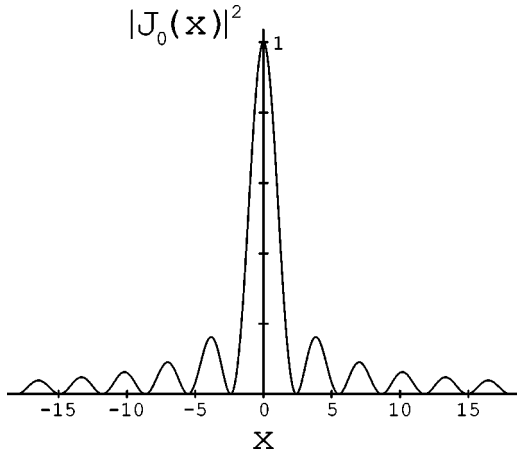


FIG. 2. Plot of $|J_0|^2$ (where J denotes a Bessel function) as a function of its argument.

knowledge of the measured state, so that the minimum number n of measuring points needed to apply the matrix inversion method must first be estimated from the graph $|\psi_0(C)|^2$, which thus has to be known with sufficient accuracy. Second, in order to minimize the impact of measurement errors on the matrix inversion process, it is important to make a judicious choice of the C values to be used for this purpose. A quick glimpse at the graph of J_0^2 in Fig. 2 readily allows us to figure out a convenient strategy. Since the central maximum $J_0^2(0) = 1$ is very pronounced, one expects that by choosing

$$C_\mu \equiv \mu Q, \quad (23)$$

the approximation $|\psi_0(C_\mu)|^2 \approx |w_\mu|^2$ will be a good one as long as $Q/2$ is larger than the central peak's width. In our simulations we use the value¹ $Q=7$. In Fig. 3(a), the expected signal $|\psi_0(C)|^2$ is shown for a quantum field prepared in a coherent state with $\langle a^\dagger a \rangle = 6$. Even without further calculations, the Poissonian photon-number distribution can be immediately inferred from this graph by simple inspection. A second example is shown in Fig. 3(b), which shows a corresponding curve for an arbitrary superposition of Fock states ($|w_0|^2=0.1$, $|w_1|^2=0.15$, $|w_2|^2=0.25$, $|w_3|^2=0.3$, $|w_4|^2=0.2$). Also here the main peaks already allow a crude estimation of the photon-number distribution and, therefore, of the minimum number n of measuring points required for the matrix inversion. As we have verified numerically, by choosing the values C_μ according to strategy (23), the inversion of Eq. (22) turns out to provide reliable values for the coefficients $|w_\nu|^2$ even if up to 10% Gaussian noise is superposed to every selected measuring point. We have also gradually reduced the value of Q and verified that the method ceases to apply for $Q < 2\pi$, because individual maxima then start to overlap and become indiscernible from each other.

¹The distance between two consecutive maxima in Fig. 2 continually decreases for larger arguments and converges asymptotically to the value 2π .

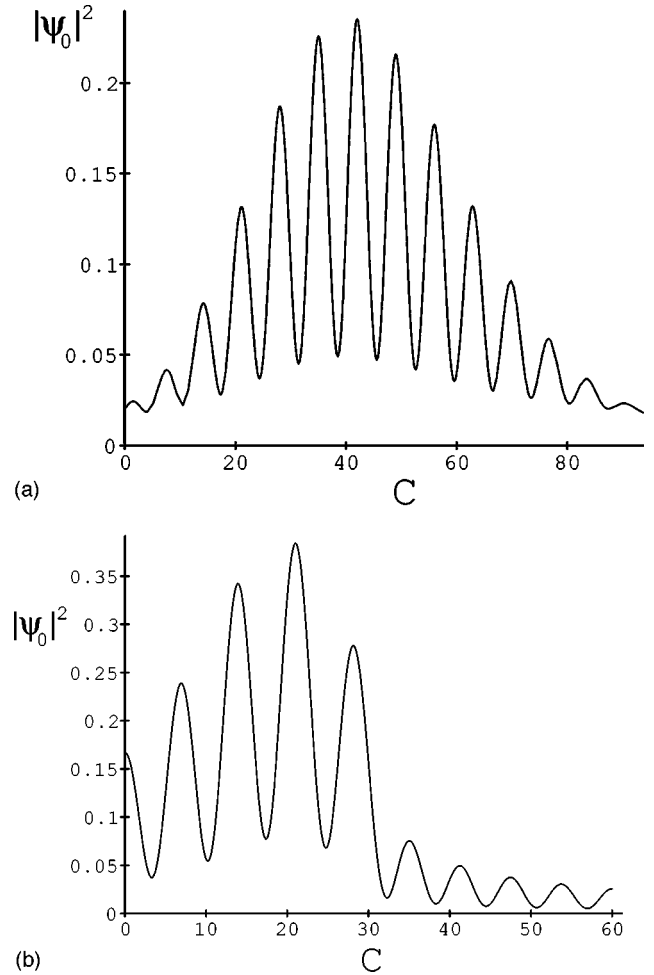


FIG. 3. Zeroth-order (undeflected) atomic flux $|\psi_0|^2$ as a function of the classical light intensity (Raman-Nath parameter C) of the second sinusoidal phase grating. In (a) the quantum field is assumed to be in a coherent state with $\langle a^\dagger a \rangle = 6$. In (b) the following photon number distribution has been assumed: $|w_0|^2=0.1$, $|w_1|^2=0.15$, $|w_2|^2=0.25$, $|w_3|^2=0.3$, and $|w_4|^2=0.2$.

In principle, the presented QND scheme could be applied in a single run. Due to cavity losses, however, the available time for the measurement is limited, and it will depend on the intensity of the atomic source, if enough atoms pass the cavity before its field has substantially decayed. The stringent requirements on atomic beam preparation (see Sec. VI) and the need to scan C over a sufficient range during the available measuring time additionally complicate the problem. Because of these technical reasons, it will probably be necessary to repeat the experience several times, with identically prepared quantum states, in order to accumulate enough data points for the method to be applicable.

V. A NULL TEST OF LIGHT QUANTIZATION

The influence of light quantization on the motion of near-resonant atoms becomes apparent in the strong-coupling regime. It is for this reason that all proposed photon-statistics measurement schemes assume coupling constants Q of the order of ~ 1 . As Q is made smaller, a quantum field behaves

more and more like a classical one. For instance, the atomic far-field diffraction pattern produced by a standing wave of light becomes nearly indistinguishable from the classically expected Kapitza-Dirac distribution. A sensitive experimental test of this statement could be performed with an atomic TI. As we already commented at the end of Sec. II, a perfectly matched TI using classical light gratings leaves an incoming atomic beam intact. In order to see how this classical limit arises, we have to leave the strong-coupling regime, in which light quantization shows up rather evidently, and assume $Q \ll 1$. The possibly most “classical” field is a coherent state,

$$|w_\nu\rangle^2 = \frac{\langle a^\dagger a \rangle^\nu}{\nu!} e^{-\langle a^\dagger a \rangle}, \quad (24)$$

with an average number $\langle a^\dagger a \rangle$ of photons. Then, if we use a common integral representation of J_l ,

$$J_l^2(x) = \frac{1}{2\pi} \int_{(2\pi)} dk \frac{1}{2\pi} \int_{(2\pi)} dk' e^{il(k-k')} e^{-ix(\sin k - \sin k')}, \quad (25)$$

the series in Eq. (21) can be summed up explicitly. The resulting expression,

$$|\psi_l|^2 = \frac{1}{2\pi} \int_{(2\pi)} dk \frac{1}{2\pi} \int_{(2\pi)} dk' e^{il(k-k')} \times e^{-i\langle a^\dagger a \rangle} e^{iC(\sin k - \sin k')/2} \exp[\langle a^\dagger a \rangle e^{-iQ(\sin k - \sin k')/2}], \quad (26)$$

can be simplified, for $Q \ll 1$ implies

$$e^{-iQ(\sin k - \sin k')/2} \simeq 1 - i \frac{Q}{2} (\sin k - \sin k'). \quad (27)$$

The matching condition

$$C = Q \langle a^\dagger a \rangle \quad (28)$$

further reduces the remaining integrals, finally giving

$$|\psi_l|^2 = \left| \frac{1}{2\pi} \int_{(2\pi)} dk e^{ilk} \right|^2 = \delta_{l,0}. \quad (29)$$

Physically speaking, the classical field exactly compensates the atomic wave-front corrugation produced by the quantum field in the weak-coupling regime $Q \ll 1$. This is precisely the expected behavior in the semiclassical limit, as expressed by the correspondence principle.

By considering more terms in the expansion (27), one is able to predict what happens beyond the classical limit. The lowest-order quantum correction is obtained by including the next higher Taylor coefficient in Eq. (27). By doing so and after inserting the matching condition (28), one gets

$$|\psi_l|^2 = \frac{1}{2\pi} \int_{(2\pi)} dk \frac{1}{2\pi} \int_{(2\pi)} dk' e^{il(k-k')} e^{-CQ(\sin k - \sin k')^2/8}. \quad (30)$$

Although the integrals may be expressed in terms of modified Bessel functions I_l , a more transparent result is obtained by assuming $CQ/8 \ll 1$, which then allows us to Taylor-expand the exponential to lowest order,

$$|\psi_l|^2 = \frac{1}{2\pi} \int_{(2\pi)} dk \frac{1}{2\pi} \int_{(2\pi)} dk' e^{il(k-k')} \times \left[1 - \frac{CQ}{8} (\sin k - \sin k')^2 \right]. \quad (31)$$

After evaluating the remaining integrals, one finds

$$|\psi_l|^2 = \delta_{l,0} [1 - CQ/8] + [\delta_{l,1} + \delta_{l,-1}] CQ/16, \quad (32)$$

i.e., the fact that light is quantized shows up in anomalous diffraction in the first and minus first orders. Without the restriction $CQ/8 \ll 1$, also higher diffraction orders would be populated. We note that Eq. (32) is consistent with respect to flux conservation, since $1 - CQ/8 + 2 \times CQ/16 = 1$. If only the deflected beam components are detected (e.g., by blocking the zeroth diffraction order), a nonzero result would be an indicator of light quantization.

If the matching condition (28) is not exactly fulfilled, the same approximation that led to Eq. (32) produces

$$|\psi_l|^2 = J_l^2 \left(\frac{C - Q \langle a^\dagger a \rangle}{2} \right) + \frac{\langle a^\dagger a \rangle Q^2}{8} \left[J_l^2 \left(\frac{C - Q \langle a^\dagger a \rangle}{2} \right) \right]', \quad (33)$$

where the primes denote derivation with respect to the argument. Equation (33) correctly reduces to the previous result (32) when the matching condition is satisfied. For $|(C - Q \langle a^\dagger a \rangle)/2| < 1.08$, the sign of $[J_0^2]'$ is negative and J_0^2 decreases monotonically. This shows that the proper tuning of C , satisfying Eq. (28), can be achieved by *maximizing* the measured atomic flux $|\psi_0(C)|^2$ into the zeroth diffraction order.

Real-life effects of different origins spoil this simple picture, of course, and even when perfectly matched, a TI will produce some diffraction away from the propagation axis z . We now proceed to study different sources of aberrations.

VI. LIMITATIONS OF THE METHOD

In our analysis, we will assume two classical ideally matched light fields of coupling constant C and see how different sources of aberrations modify the expected far-field diffraction pattern.

Most problematic is the velocity dependence of the Talbot distance,

$$D(\mathbf{v}_z) = \frac{v_z}{\langle v_z \rangle} D(\langle \mathbf{v}_z \rangle), \quad (34)$$

which gives rise to a chromatical aberration. Namely, if the TI has been adjusted with respect to the average atom velocity $\langle \mathbf{v}_z \rangle$, it will no longer be adjusted for other speeds. Our natural distance units were defined according to

$$\frac{\zeta}{2\pi} D(\langle v_z \rangle) = z. \quad (35)$$

If the relative velocity mismatch is denoted by $\epsilon \equiv \zeta[1 - \langle v_z \rangle / v_z]$, for a given distance ζ between the gratings the modified wave function, ψ_ϵ , is given by

$$\psi_\epsilon(\xi, \zeta) = e^{-i\epsilon(\partial^2/\partial\xi^2)} \psi_{\epsilon=0}(\xi, \zeta). \quad (36)$$

At the exit of the second light grating, the ϵ -modified wave function then reads

$$\psi_\epsilon(\xi, \pi) = e^{iC\sin^2(\xi/2)} e^{-i\epsilon(\partial^2/\partial\xi^2)} e^{iC\cos^2(\xi/2)}. \quad (37)$$

To lowest order in ϵ , Eq. (37) is evaluated to be

$$\psi_\epsilon(\xi, \pi) = e^{iC} \left\{ 1 + i\epsilon \left[\frac{1}{2} \left(\frac{C}{2} \right)^2 + \frac{C}{2} \cos \xi - \left(\frac{C}{2} \right)^2 \cos(2\xi) \right] \right\}. \quad (38)$$

In this form, the Fourier decomposition of the wave front ψ_ϵ can be directly read off. Inasmuch as the Fourier components correspond to the far-field diffraction amplitudes, we conclude that for a realistical ϵ of the order of 1%, the parameter C should be of the order of unity, if diffraction into nonzero orders is to be kept at the percent level. For this reason, the assumption $CQ/8 \ll 1$ that eventually led to Eqs. (32) and (33) in the preceding section is *a posteriori* well justified in the weak-coupling regime and under realistic experimental conditions.

The reason why values $C \gg 1$ are inadequate for a practical realization of the proposed null-measurement experiment becomes evident as soon as one plots the diffraction near field produced by gratings of the form (3) for various values of C [16,27]. As soon as $C > \pi/2$, the diffraction patterns become increasingly complex and depend more and more sensibly on the distance z behind the grating. Even for a monochromatic atomic beam, misadjustment of the distance $D/2$ leads to spurious diffraction into nonzero orders. The mathematics is the same as above, only now ‘‘ ϵ ’’ refers to the positioning error of the second grating, $\psi(\xi, \pi + \epsilon)$. For Talbot distances in the 10^{-2} m regime, a relative positioning precision of 1% should not represent major technical problems.

For the proposed QND measurement scheme, on the other hand, larger off-beam deflections may be tolerated. Still, C values of the magnitude shown in Figs. 3(a) and 3(b) are probably unrealistically large in view of the above results. In a real experiment, one would either be limited to small photon numbers or the ideal choice $Q \approx 7$ will have to be abandoned. In fact, such a large coupling constant is a challenge in itself, even in view of the extreme values reported in recent works [28]. Smaller Q values lead to larger errors when the simple inversion method of Sec. IV is applied. In that case, numerical fitting to the measured $|\psi_0(C)|^2$ curve will be necessary as a second step.

Also the angular alignment of the gratings must be kept under strict control. A thorough theoretical and experimental analysis of the required precision can be found

in Ref. [22] for a single grating. The essential result is that the parameter C gets multiplied by a Gaussian factor $\exp[-(2\pi i_{\text{int}} v_{\parallel})^2 / 2\lambda^2]$, where v_{\parallel} is the atomic velocity component along the tilted grating axis. Ideally, the orthogonality of the atomic beam with respect to the grating axes should be so precise that the induced change in C is not larger than other inherent variations of C , such as produced by laser intensity fluctuations and frequency drifts. Note, however, that as long as this tilting angle is identical for the two light fields, the TI matching condition itself is not spoiled. The strictly parallel position may be actively controlled with an additional optical interferometer [29] or by mounting the quantum cavity and the retroreflection mirror on a common structure with a low thermal expansion coefficient [30]. A parallel light field alignment of the order of 10^{-5} rad has been reported in [31].

Another important problem is posed by the finite entrance aperture of the TI. The number of grating periods the atoms should ‘‘see’’ must be chosen large enough for two reasons. First, the fidelity of a Talbot image depends on the length over which the grating is illuminated. Second, the width of the diffracted beamlets should be much smaller than the lateral distance between them. The ratio between these quantities is approximately given by $d/(\lambda/2)$. If the diffraction orders cannot be clearly separated in the far field, both the QND measurement scheme and the light quantization null-test method break down. The fidelity problem is the more severe one, since a crude estimate of the necessary minimum number of comprised grating periods gives $d/(\lambda/2) \approx 20$ [15]. A recent numerical and experimental study confirms this [32]. For such a large value, the far-field diffraction orders would be already well separated. Since the geometry of a high-quality factor optical cavity possibly restricts the number of usable light intensity periods, it could be experimentally convenient to place the classical field *before* the quantum field. From the symmetry of Eq. (21) under $C \leftrightarrow \nu Q$ it is clear that such an inversion does not alter the measured diffraction intensities. Atomic wave fronts with the required lateral extent and coherence can be created by appropriate slit collimation. For instance, a width $d = 5 \mu\text{m}$ is used in the Innsbruck three-grating argon interferometer [31]. This approximately corresponds to 20 grating periods, if sodium is used instead of argon. At the expense of atomic flux, even broader beams may be produced. Note, however, that the mandatory fulfillment of the far-field condition $z \gg d^2/\lambda_{dB}$ may lead to prohibitive interferometer lengths.

A further point we want to make is the influence of spontaneous-emission processes. In the context of atom diffraction by light, these have been studied in detail, both experimentally and theoretically [33–35]. An easy way to suppress them is by using large enough detunings [31]. We want to stress that atomic Talbot interferometry may also prove useful to study the limit between the diffractive and the diffusive scattering regime. If two classical light fields produced by the same source form an atomic TI, which has been matched in the diffractive limit, a gradual reduction of the detuning will lead to atomic deflections away from the beam propagation axis z , and this effect will be solely due to spontaneous diffusion. This is another example in which a TI may

help to filter out the information one is specifically interested in. In this sense, what would be an aberration for a quantum measurement could become an interesting signal when a different phenomenon is being studied.

As another example of this general observation, let us consider the situation in which the atomic ground state is split into a nondegenerate multiplet of sublevels. If the atom is in an arbitrary superposition of these states, this would imply that each component is differently detuned from the upper (excited) level. Since the Raman-Nath parameter C of the atom-grating interaction is inversely proportional to the detuning from a given transition, the TI can only be matched for *one* of the ground-state sublevels. Experimentally this problem can be circumvented using optical pumping techniques, thus leading to a true two-level system. Alternatively, a TI could be used to *measure* the populations of the various atomic ground-state sublevels. Mathematically, the situation is analogous to Eq. (21), with the role of the infinite number of $|w_\nu|^2$ coefficients replaced by the finite number of sublevel population probabilities. A recent example in which such a measurement could be useful is given in Ref. [36].

In conclusion, it should be technically feasible (although experimentally challenging) to build a phase-grating atomic TI which deflects not more than a few percent of the incoming atomic intensity away from the propagation axis. Such a device would satisfy the requirements imposed by our proposed cavity quantum electrodynamical experiments. The elimination of any kind of aberrations is especially important

when the device is used as a null instrument, and it determines its final sensitivity. With off-beam deflections reduced to the percent level, quantum signatures $1 - |\psi_0|^2 = QC/8$ of the same order of magnitude should be detectable. A realistic choice of parameters, for instance $C = 5$ and $Q = 1/60$, would allow us to demonstrate the quantum nature of a light field of about 300 photons.

VII. SUMMARY

The potential usefulness of atomic Talbot interferometrical methods for the purpose of cavity quantum electrodynamical measurements is studied. An alternative QND scheme for the determination of the photon-number distribution of an arbitrary light state is discussed. Its range of applicability is shown to critically depend on the magnitude C of the Raman-Nath factor, for which the TI can be matched with the required precision.

Also, a light-quantization detector based on measurable departures from a zero result expected in the classical limit is proposed. We show that its construction should be feasible using state-of-the-art techniques.

ACKNOWLEDGMENTS

This work was supported by the Conselho Nacional de Desenvolvimento Científico e Tecnológico (CNPq) and the Latin American Center for Physics (CLAF).

-
- [1] P. Meystre, E. Schumacher, and S. Stenholm, *Opt. Commun.* **73**, 443 (1989).
 - [2] V.M. Akulin, Fam Le Kien, and W.P. Schleich, *Phys. Rev. A* **44**, R1462 (1991).
 - [3] M.J. Holland, D.F. Walls, and P. Zoller, *Phys. Rev. Lett.* **67**, 1716 (1991).
 - [4] S. Haroche, M. Brune, and J.M. Raimond, *Appl. Phys. B: Photophys. Laser Chem.* **54**, 355 (1992).
 - [5] A.M. Herkommer, V.M. Akulin, and W.P. Schleich, *Phys. Rev. Lett.* **69**, 3298 (1992).
 - [6] M. Freyberger and A.M. Herkommer, *Phys. Rev. Lett.* **72**, 1952 (1994).
 - [7] P. Domokos, P. Adam, J. Janszky, and A. Zeilinger, *Phys. Rev. Lett.* **77**, 1663 (1996).
 - [8] R. Walser, J.I. Cirac, and P. Zoller, *Phys. Rev. Lett.* **77**, 2658 (1996).
 - [9] B. Rohwedder, L. Davidovich, and N. Zagury, *Phys. Rev. A* **60**, 480 (1999).
 - [10] See M. Brune, F. Schmidt-Kaler, A. Maali, J. Dreyer, E. Hagley, J.M. Raimond, and S. Haroche, *Phys. Rev. Lett.* **76**, 1800 (1996), and references therein.
 - [11] I.Sh. Averbukh, V.M. Akulin, and W.P. Schleich, *Phys. Rev. Lett.* **72**, 437 (1994).
 - [12] B. Rohwedder and M. Orszag, *Phys. Rev. A* **54**, 5076 (1996).
 - [13] At $z = D/2$, a self-image is formed which is laterally displaced by half a grating period. For this reason it cannot be properly interpreted as a ‘‘shadow’’ of the grating.
 - [14] W.H. Fox Talbot, *Philos. Mag.* **9**, 401 (1836).
 - [15] K. Patorski, in *Progress in Optics*, edited by E. Wolf (North-Holland, Amsterdam, 1989), Vol. 27. See, in particular, paragraph 2.6.2.
 - [16] B. Rohwedder, *Fortschr. Phys.* **47**, 883 (1999).
 - [17] A.W. Lohmann and D.E. Silva, *Opt. Commun.* **2**, 413 (1971).
 - [18] J.F. Clauser and S. Li, *Phys. Rev. A* **49**, R2213 (1994).
 - [19] M.S. Chapman, C.R. Ekstrom, T.D. Hammond, J. Schmiedmayer, B.E. Tannian, S. Wehinger, and D.E. Pritchard, *Phys. Rev. A* **51**, R14 (1995).
 - [20] J.F. Clauser and S. Li, in *Atom Interferometry*, edited by P. Berman (Academic, New York, 1997).
 - [21] P.L. Gould, G.A. Ruff, and D.E. Pritchard, *Phys. Rev. Lett.* **56**, 827 (1986).
 - [22] P.J. Martin, P.L. Gould, B.G. Oldaker, A.H. Miklich, and D.E. Pritchard, *Phys. Rev. A* **36**, 2495 (1987).
 - [23] B. Rohwedder (unpublished).
 - [24] S. Dyrting and G.J. Milburn, *Phys. Rev. A* **49**, 4180 (1994), and references therein.
 - [25] The spatial profile of a typical standing wave of light is Gaussian. In the purely diffractive regime that we are considering here, this fact can be taken into account simply by multiplying the Raman-Nath parameter by a geometrical factor $\sqrt{\pi/2}$ [22,31].
 - [26] R.M.S. Knops, Ph. D. thesis, Technische Universiteit Eindhoven (1998).
 - [27] B. Rohwedder, The Australian National University internal re-

- port (1996) (unpublished). Copies can be requested from the author.
- [28] C.J. Hood, M.S. Chapman, T.W. Lynn, and H.J. Kimble, *Phys. Rev. Lett.* **80**, 4157 (1998).
- [29] G. Timp, R.E. Behringer, D.M. Tennant, J.E. Cunningham, M. Prentiss, and K.K. Berggren, *Phys. Rev. Lett.* **69**, 1636 (1992).
- [30] J.J. McClelland, R.E. Scholten, E.C. Palm, and R.J. Celotta, *Science* **262**, 877 (1993).
- [31] E.M. Rasel, M.K. Oberthaler, H. Batelaan, J. Schmiedmayer, and A. Zeilinger, *Phys. Rev. Lett.* **75**, 2633 (1995).
- [32] R. Moignard and J.L. de Bougrenet, *Opt. Commun.* **132**, 41 (1996). In this reference the quality of Talbot images produced by binary gratings is studied. The self-imaging fidelity is enhanced if smooth gratings (such as the one we are considering here) are used instead.
- [33] P.L. Gould, P.J. Martin, G.A. Ruff, R.E. Stoner, J.-L. Picqué, and D.E. Pritchard, *Phys. Rev. A* **43**, 585 (1991).
- [34] S.M. Tan and D.F. Walls, *Phys. Rev. A* **44**, R2779 (1991).
- [35] S.M. Tan and D.F. Walls, *Appl. Phys. B: Photophys. Laser Chem.* **54**, 434 (1992).
- [36] É. Maréchal, S. Guibal, J.-L. Bossennec, M.-P. Gorza, R. Barbé, J.-C. Keller, and O. Gorceix, *Eur. Phys. J. D* **2**, 195 (1998).